AIAA SciTech Forum
7-11 January 2019, San Diego, California
AIAA Scitech 2019 Forum

10.2514/6.2019-1027

Dynamic Analysis of Laminated Composite Plate Using Non-Polynomial Shear Deformation Theory Under Hygrothermal Environment

B. R.Thakur*, S. Verma †, B.N.Singh‡ and D.K.Maiti§
Indian Institute of Technology Kharagpur, West Bengal 721302, India.

A nine-noded isoparametric finite element formulation based on the non-polynomial shear deformation theory (NPSDT) is presented for the transient analysis of laminated composite plate subjected to hygrothermal environment. In this study, inverse hyperbolic type of non-polynomial shear deformation theory is considered which provides nonlinear distribution of transverse shear stresses, and also satisfy the traction-free boundary conditions at the top and bottom surfaces of the laminates. A generalized thermoelastic stress-strain relation is considered to derive the governing equation using Hamilton's principle. Newmark's direct integration scheme is used to solve the dynamic equation of equilibrium at every time step during the transient analysis. Several numerical examples are considered and the results are compared with those available in the literature. The effect of various parameters on the transient response of laminated composite plate under hygrothermal environment have been investigated. The work reported in this paper provides an efficient modeling approach for thermal vibration analysis of laminated composite plates in practical engineering.

I. Introduction

Composite materials are being increasingly used in aerospace and other structural applications because of their specific quality like low density, high strength, high stiffness, ease in fabrication and excellent thermal characteristics. During the operational life, the variation of temperature and moisture reduces the elastic moduli of the material and induces internal initial stresses, which may affect the stability as well as the safety of the structures. As a result, a careful evaluation of the effects of environmental exposure is required to find the nature and extent of their deleterious effects upon performance.

The changes in dynamic characteristics due to the hygrothermal effect seem to be an important consideration in composite analysis and design, which are of practical interest. Numerous analytical studies for vibration analysis of laminated composite plate in thermal environments have been presented using the equivalent single layer theory, zigzag theory and layerwise theory. The effect of environment on the free vibration of laminated plates was studied by Whitney and Ashton [1]. They used the Ritz method to analyze symmetric laminates and equilibrium equations of motion based on the classical laminated plate theory for finding the natural frequencies of simply supported plates subjected to moisture and temperature effect. Sai Ram and Sinha [2] investigated the effects of moisture and temperature on the free vibration of laminated composite plates using the first order shear deformation theory (FSDT). Results were presented showing the reduction in the natural frequency with the increase in uniform moisture concentration and temperature for different laminates with varying boundary conditions. Patel et al. [3] developed a C^0 eight-noded quadrilateral plate element based on a high-order zigzag theory for static and dynamic analysis of thick laminated composite plates in hygrothermal environments. Rao and Sinha [4] developed a 20-noded hexahedral isoparametric element in order to study the effects of the moisture and temperature on the dynamic response of multidirectional composite plates. Singha et al. [5] adopted a four-noded quadrilateral plate element based on the first order shear deformation theory to study the small amplitude vibration characteristics of thermally stressed composite skew plate. Rath and Sahu [6] adopted an eight-noded isoparametric plate element based on the first order shear deformation theory to perform a free vibration analysis of woven fiber laminated composite plates in hygrothermal environment. Li et al. [7] utilized the first order shear deformation theory to study the vibration and sound radiation response of asymmetric rectangular

*Research Scholar, Department of Aerospace Engineering, brt.iitkgp@gmail.com and AIAA Student Member.
†Research Scholar, Department of Aerospace Engineering, surendraverma2501@gmail.com and AIAA Student Member.
‡Professor, Department of Aerospace Engineering, bnsingh@aero.iitkgp.ernet.in
§Professor, Department of Aerospace Engineering, dkmaiti@aero.iitkgp.ernet.in

laminated plates in thermal environments. Parhi et al.[8] investigated the effects of moisture and temperature on the dynamic behavior of composite laminated plates and shells with or without delaminations based on FSDT. The effects of hygrothermal conditions on the dynamic response of shear deformable laminated plates resting on elastic foundations has been investigated by Shen et al. [9]. Recently, few papers on transient analysis have been reported by researcher's [10–12] but to the best of authors' knowledge, no work has been reported so far in open literature on transient analysis of laminated composite plates using nonpolynomial shear deformation theory in hygrothermal environment.

The present work based on nonpolynomial shear deformation theory (NPSDT) given by Grover et al. [13] which takes account of transverse shear effects of the laminate and satisfy the zero transverse shear stress boundary condition over top and bottom surfaces of the plate. A computationally efficient C^0 finite element methodology is applied to examine the free vibration and transient response of laminated composite plate under hygrothermal effect using inverse hyperbolic shear deformation theory (IHSDT). There is hardly any research paper available in the open literature which uses non-polynomial shear deformation theory for the transient analysis of laminate composite under thermal loading. Hence, this paper try to give extensive and detail analysis of transient behavior of laminate composite under the consideration of different mechanical and thermal load.

II. Mathematical Formulation

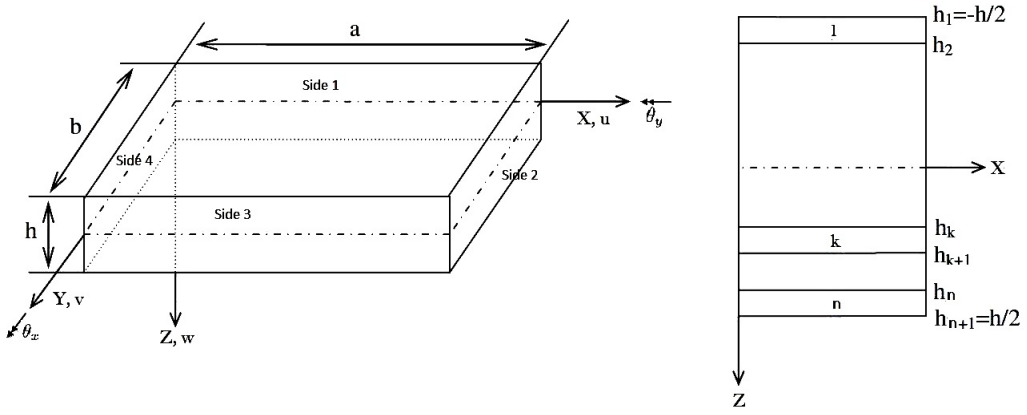

Fig. 1 Schematic diagram of laminated composite plate.

A composite laminated plate is considered with the Cartesian coordinates X, Y along the in-plane directions, and Z along the thickness direction as shown in Fig.1. The non-polynomial shear deformation theory (NPSDT) used in the present analysis is inverse hyperbolic shear deformation theory (IHSDT), developed by Grover et al.[13]. The displacement field model can be expressed as follows

$$\begin{aligned} u(x,y,z) &= u_0(x,y) - z\frac{\partial w_0}{\partial x} + f(z)\,\theta_x(x,y) \\ v(x,y,z) &= v_0(x,y) - z\frac{\partial w_0}{\partial y} + f(z)\,\theta_y(x,y) \\ w(x,y,z) &= w_0(x,y) \end{aligned} \tag{1}$$

where u_0, v_0, w_0 are the mid plane displacements, θ_x, θ_y are the shear deformations at the mid plane. The function $f(z) = (g(z) + z\Omega)$ represent the warping of the cross-section perpendicular to mid-plane, in which $g(z) = sinh^{-1}\left(\frac{rz}{h}\right)$ and $\Omega = \frac{-2r}{h\sqrt{r^2+4}}$. The parameter $r = 3$ is the transverse shear stress parameter and h is the plate thickness.

The state-of-strain at a point corresponding to IHSDT displacement field is expressed as

$$\{\epsilon_l\} = \begin{Bmatrix} \frac{\partial u}{\partial x} \\ \frac{\partial v}{\partial y} \\ \frac{\partial u}{\partial y} + \frac{\partial v}{\partial x} \\ \frac{\partial v}{\partial z} + \frac{\partial w}{\partial y} \\ \frac{\partial u}{\partial z} + \frac{\partial w}{\partial x} \end{Bmatrix} = \begin{bmatrix} \frac{\partial}{\partial x} & 0 & -z\frac{\partial^2}{\partial x^2} & f(z)\frac{\partial}{\partial x} & 0 \\ 0 & \frac{\partial}{\partial y} & -z\frac{\partial^2}{\partial y^2} & 0 & f(z)\frac{\partial}{\partial y} \\ \frac{\partial}{\partial x} & \frac{\partial}{\partial y} & -2z\frac{\partial^2}{\partial x \partial y} & f(z)\frac{\partial}{\partial x} & f(z)\frac{\partial}{\partial y} \\ 0 & 0 & 0 & 0 & f'(z) \\ 0 & 0 & 0 & f'(z) & 0 \end{bmatrix} \begin{Bmatrix} u_0 \\ v_0 \\ w_0 \\ \theta_x \\ \theta_y \end{Bmatrix} \tag{2}$$

The presence of second order derivative operator in Eq. 2 requires C^1 continuity in field variable w_0. The use of Lagrangian element in the finite element analysis gives at most C^0 continuity of field variables. Hence the reduction of C^1 to C^0 continuity is done by imposing artificial constraint as $\partial w_0/\partial x = \phi_x$ and $\partial w_0/\partial y = \phi_y$ which leads to seven degree of freedom. The displacement equations after imposing constraints are given as

$$\begin{Bmatrix} u \\ v \\ w \end{Bmatrix} = \begin{bmatrix} 1 & 0 & 0 & -z & 0 & f(z) & 0 \\ 0 & 1 & 0 & 0 & -z & 0 & f(z) \\ 0 & 0 & 1 & 0 & 0 & 0 & 0 \end{bmatrix} \begin{Bmatrix} u_0 \\ v_0 \\ w_0 \\ \phi_x \\ \phi_y \\ \theta_x \\ \theta_y \end{Bmatrix} = [Z]\{q\} \tag{3}$$

The generalized thermoelastic stress-strain relations under plain stress condition for an arbitrary layer k are given by the following equations

$$\{\sigma\}_k = \left[R_{(k)}\right][Q]_k \left[R_{(k)}\right]^T \left(\{\epsilon_l\}_k - \{\epsilon_{th}\}\right) = \left[\bar{Q}\right]_k \left(\{\epsilon_l\}_k - \{\alpha\}_k \Delta T - \{\beta\}_k \Delta C\right) \tag{4}$$

which can be elaborately written as

$$\begin{Bmatrix} \sigma_x \\ \sigma_y \\ \tau_{xy} \\ \tau_{yz} \\ \tau_{xz} \end{Bmatrix}_{(k)} = \left[R_{(k)}\right] \begin{bmatrix} Q_{11} & Q_{12} & Q_{16} & 0 & 0 \\ Q_{21} & Q_{22} & Q_{26} & 0 & 0 \\ Q_{61} & Q_{62} & Q_{66} & 0 & 0 \\ 0 & 0 & 0 & Q_{44} & Q_{45} \\ 0 & 0 & 0 & Q_{54} & Q_{55} \end{bmatrix} \left[R_{(k)}\right]^T \left(\begin{Bmatrix} \epsilon_x \\ \epsilon_y \\ \gamma_{xy} \\ \gamma_{yz} \\ \gamma_{xz} \end{Bmatrix}_{(k)} - \Delta T \begin{Bmatrix} \alpha_x \\ \alpha_y \\ \alpha_{xy} \\ 0 \\ 0 \end{Bmatrix}_{(k)} - \Delta C \begin{Bmatrix} \beta_x \\ \beta_y \\ \beta_{xy} \\ 0 \\ 0 \end{Bmatrix}_{(k)} \right) \tag{5}$$

in which, $\{\sigma\}_k$, $\{\epsilon\}_k$ and $\left[\bar{Q}\right]_k$ are stress vector, strain vector and the materials matrix for the k^{th} lamina in global coordinate system, respectively. Where, $\{\alpha\}_k$ and $\{\beta\}_k$ are the thermal expansion coefficients and moisture coefficient vector, respectively.The local-to-global transformation matrix is represented by $[R]$. The ΔT and ΔC represent the rise in temperature and moisture concentration, respectively.

Each material matrix coefficient can be expressed as

$$Q_{11} = \frac{E_1}{1-\nu_{12}\nu_{21}}, Q_{12} = \frac{\nu_{12}E_2}{1-\nu_{12}\nu_{21}}, Q_{22} = \frac{E_2}{1-\nu_{12}\nu_{21}}, Q_{66} = G_{12}, Q_{44} = G_{23}, Q_{55} = G_{13}$$

The Longitudinal and transverse direction are defined by 1 and 2 respectively. Above, E_1 and E_2 are the Young's modulus; G_{12}, G_{23}, and G_{13} are the shear modulus; and ν_{12} and ν_{21} are major and minor Poisson ratios.

The governing equations of motion of the system for the dynamic analysis of plate are derived using Hamilton's principle and the same is expressed as follows

$$\delta \int_{t_i}^{t_f} \mathcal{L} dt = \int_{t_i}^{t_f} \left(\delta K - \delta U - \delta U_\gamma + \delta W\right) dt = 0 \tag{6}$$

Where, K is the kinetic energy of the system, U is the total strain energy of the system, W is the work done by the external force and U_γ is the strain energy due to the imposition of artificial constraint. The 1^{st} term of Eq. 6 is represented by

$$\delta K = -\int_{\Omega} \delta \{q\}^T [m] \{\ddot{q}\} \, d\Omega \tag{7}$$

where $[m]$ is the mass matrix which is given by

$$[m] = \int \rho [Z]^T [Z] \, dz$$

in which ρ is the density per unit volume.

The 2^{nd} term of Eq. 6 is the strain energy due to the linear strain vector and initial stress generated by hygrothermal load and given by

$$\delta U = \frac{1}{2} \int_V \left(\delta \{\epsilon_l\}^T \{\sigma\} + \delta \{\epsilon_{nl}\}^T \{\sigma'\} \right) dz d\Omega = \delta U_1 + \delta U_2 \tag{8}$$

where $\{\epsilon_l\}$ is the linear component of strain vector, $\{\epsilon_{nl}\}$ is the nonlinear component of strain vector and $\{\sigma'\}$ is the residual stress vector due to hygrothermal load.

Following the Green-Lagrange strain relation, the nonlinear strain vector, $\{\epsilon_{nl}\}$ is expressed as

$$\{\epsilon_{nl}\} = \begin{Bmatrix} \frac{1}{2}\left\{\left(\frac{\partial u}{\partial x}\right)^2 + \left(\frac{\partial v}{\partial x}\right)^2 + \left(\frac{\partial w}{\partial x}\right)^2\right\} \\ \frac{1}{2}\left\{\left(\frac{\partial u}{\partial y}\right)^2 + \left(\frac{\partial v}{\partial y}\right)^2 + \left(\frac{\partial w}{\partial y}\right)^2\right\} \\ \frac{\partial u}{\partial x}.\frac{\partial u}{\partial y} + \frac{\partial v}{\partial x}.\frac{\partial v}{\partial y} + \frac{\partial w}{\partial x}.\frac{\partial w}{\partial y} \\ \frac{\partial u}{\partial y}.\frac{\partial u}{\partial z} + \frac{\partial v}{\partial y}.\frac{\partial v}{\partial z} + \frac{\partial w}{\partial y}.\frac{\partial w}{\partial z} \\ \frac{\partial u}{\partial x}.\frac{\partial u}{\partial z} + \frac{\partial v}{\partial x}.\frac{\partial v}{\partial z} + \frac{\partial w}{\partial x}.\frac{\partial w}{\partial z} \end{Bmatrix} \tag{9}$$

The above nonlinear strain vector, $\{\epsilon_{nl}\}$ can be rewritten by substituting Eq. 3 in Eq. 9 as

$$\{\epsilon_{nl}\} = [R] \left\{\theta_g\right\}$$

where $[R]$ is the multiplier matrix, obtained following the procedure given in the Ref. [8] and $\left\{\theta_g\right\}$ is the generalized strain vector, which can be expressed as

$$\left\{\theta_g\right\}^T = \left\{ \begin{array}{cccccccccccccc} \frac{\partial u_0}{\partial x} & \frac{\partial v_0}{\partial y} & \frac{\partial u_0}{\partial y} + \frac{\partial v_0}{\partial x} & \frac{\partial \phi_x}{\partial x} & \frac{\partial \phi_y}{\partial y} & \frac{\partial \phi_x}{\partial y} + \frac{\partial \phi_y}{\partial x} & \frac{\partial \theta_x}{\partial x} & \frac{\partial \theta_y}{\partial y} & \frac{\partial \theta_x}{\partial y} + \frac{\partial \theta_y}{\partial x} & \frac{\partial w_0}{\partial y} - \phi_y & \frac{\partial w_0}{\partial x} - \phi_x & \phi_y & \phi_x \end{array} \right\} \tag{10}$$

By substituting Eq. 10 in Eq. 8, the virtual strain energy, δU_2 can be obtained as

$$\delta U_2 = \int_{\Omega} \delta \left\{\theta_g\right\}^T [S] \left\{\theta_g\right\} d\Omega \tag{11}$$

where $[S]$ is the residual stress resultant matrix of dimension 13×13 and the full expression is given in the Appendix.

By substituting Eq. 3 in Eq. 2, $\{\epsilon_l\}$ can be rewritten as

$$\{\epsilon_l\} = [H] \left\{\theta_g\right\} \tag{12}$$

in which

$$[H] = \begin{bmatrix} 1 & 0 & 0 & -z & 0 & 0 & f(z) & 0 & 0 & 0 & 0 & 0 & 0 \\ 0 & 1 & 0 & 0 & -z & 0 & 0 & f(z) & 0 & 0 & 0 & 0 & 0 \\ 0 & 0 & 1 & 0 & 0 & -z & 0 & 0 & f(z) & 0 & 0 & 0 & 0 \\ 0 & 0 & 0 & 0 & 0 & 0 & 0 & 0 & 0 & 1 & 0 & f'(z) & 0 \\ 0 & 0 & 0 & 0 & 0 & 0 & 0 & 0 & 0 & 0 & 1 & 0 & f'(z) \end{bmatrix}$$

where z is the coordinate in the thickness direction and $f'(z)$ indicated the first derivative of the $f(z)$. By substituting Eq. 12 and Eq. 4 in Eq. 8, the virtual strain energy, δU_1 can be obtained as

$$\delta U_1 = \int_\Omega \delta \left\{\theta_g\right\}^T [D] \left\{\theta_g\right\} d\Omega - \int_\Omega \delta \left\{\theta_g\right\}^T \left\{\hat{F}_{th}\right\} \Omega \tag{13}$$

in which

$$[D] = \int_{-h/2}^{h/2} [H]^T \left[\bar{Q}\right] [H] \, dz \quad \text{and} \quad \left\{\hat{F}_{th}\right\} = \int_{-h/2}^{h/2} [H]^T \left[\bar{Q}\right] \{\epsilon_{th}\} \, dz$$

The strain energy due to artificial constraints, δU_γ can be expressed in terms of penalty parameter, γ, generaly taken of order 10^8, as

$$\delta U_\gamma = \frac{\gamma}{2} \int_\Omega \left\{ \delta \left(\phi_x - \frac{\partial w_0}{\partial x}\right)^T \left(\phi_x - \frac{\partial w_0}{\partial x}\right) + \delta \left(\phi_y - \frac{\partial w_0}{\partial y}\right)^T \left(\phi_y - \frac{\partial w_0}{\partial y}\right) \right\} h d\Omega \tag{14}$$

The work done by external transverse load, $P(x, y)$, can be expressed as

$$\delta W = \int_\Omega (\delta w_0 P) \, d\Omega \tag{15}$$

For nine noded finite element domain, the field variable and element geometry of the plate can be expressed in terms of interpolation functions as

$$\{q\} = \sum_{i=1}^{9} N_i \{q_i\}; \;\; x = \sum_{i=1}^{9} N_i x_i; \;\; y = \sum_{i=1}^{9} N_i y_i \tag{16}$$

where, $\{q_i\}$ is the field variable vector corresponding to i^{th} node and N_i represents the interpolation function [14].

Using Eq. 7, 11, 13, 14, 15 in Eq. 6 and utilizing Eq. 16, the discretized equations for a finite element domain can be obtained as

$$[M] \left\{\ddot{d}\right\} + \left[K + K_\gamma + K_\sigma\right] \{d\} - \{F_{th}\} = \{F_P\} \tag{17}$$

in which $[M]$ is the mass matrix, $[K]$ is the structural stiffness matrix, $\left[K_\gamma\right]$ is the stiffness due to artificial constraint, $\left[K_g\right]$ is the stiffness matrix raised due to the residual thermal stress, $\{F_P\}$ is the applied mechanical load vector, $\{F_{\Delta T} + F_{\Delta C}\}$ is the hygrothermal load vector and $\{d\}$ is the elemental displacement vector of dimension 63×1.

The expression of mass matrix, $[M]$ in Eq. 17 is obtained using Eq. 7 and Eq. 16 and given as

$$[M] = \int_\Omega [\mathcal{N}]^T [m] [\mathcal{N}] \, d\Omega$$

in which

$$\{q\} = \sum_{i=1}^{9} [\mathcal{N}_i] \{q_i\} = [\mathcal{N}] \{d\}$$

above

$$[\mathcal{N}] = \begin{bmatrix} N_i & 0 & 0 & 0 & 0 & 0 & 0 \\ 0 & N_i & 0 & 0 & 0 & 0 & 0 \\ 0 & 0 & N_i & 0 & 0 & 0 & 0 \\ 0 & 0 & 0 & N_i & 0 & 0 & 0 \\ 0 & 0 & 0 & 0 & N_i & 0 & 0 \\ 0 & 0 & 0 & 0 & 0 & N_i & 0 \\ 0 & 0 & 0 & 0 & 0 & 0 & N_i \end{bmatrix}$$

and

$$\{d\} = \left[\{q_1\}^T, \{q_2\}^T, \{q_3\}^T, \{q_4\}^T, \{q_5\}^T, \{q_6\}^T, \{q_7\}^T, \{q_8\}^T, \{q_9\}^T\right]^T$$

The total stiffness matrix, $\left[K + K_\gamma + K_\sigma\right]$ in Eq. 17 can be calculated as summation of structural stiffness, stiffness due to constraint, and initial stress stiffness as follows

$$[K] = \int_\Omega [\mathcal{B}]^T [D] [\mathcal{B}] \, d\Omega$$

in which

$$[\mathcal{B}]\{d\} = \sum_{i=1}^{9} [\mathcal{B}_i]\{q_i\}$$

where

$$[\mathcal{B}_i] = \begin{bmatrix} N_{i,x} & 0 & 0 & 0 & 0 & 0 & 0 \\ 0 & N_{i,y} & 0 & 0 & 0 & 0 & 0 \\ N_{i,y} & N_{i,x} & 0 & 0 & 0 & 0 & 0 \\ 0 & 0 & 0 & N_{i,x} & 0 & 0 & 0 \\ 0 & 0 & 0 & 0 & N_{i,y} & 0 & 0 \\ 0 & 0 & 0 & N_{i,y} & N_{i,x} & 0 & 0 \\ 0 & 0 & 0 & 0 & 0 & N_{i,x} & 0 \\ 0 & 0 & 0 & 0 & 0 & 0 & N_{i,y} \\ 0 & 0 & 0 & 0 & 0 & N_{i,y} & N_{i,x} \\ 0 & 0 & N_{i,y} & 0 & -N_i & 0 & 0 \\ 0 & 0 & N_{i,x} & -N_i & 0 & 0 & 0 \\ 0 & 0 & 0 & 0 & 0 & 0 & N_i \\ 0 & 0 & 0 & 0 & 0 & N_i & 0 \end{bmatrix}$$

similarly, penalty stiffness matrix, $\left[K_\gamma\right]$ can be expended as

$$\left[K_\gamma\right] = \int_\Omega \left[\mathcal{B}_\gamma\right]^T \begin{bmatrix} \gamma & 0 \\ 0 & \gamma \end{bmatrix} \left[\mathcal{B}_\gamma\right] d\Omega$$

in which

$$\left[\mathcal{B}_\gamma\right]\{d\} = \sum_{i=1}^{9} \left[\mathcal{B}_{\gamma i}\right]\{q_i\}$$

where

$$\left[\mathcal{B}_{\gamma i}\right] = \begin{bmatrix} 0 & 0 & N_{i,y} & 0 & 0 & 0 & -N_i \\ 0 & 0 & N_{i,x} & 0 & 0 & -N_i & 0 \end{bmatrix}$$

finally, initial stress stiffness matix, $[K_\sigma]$, can be written as

$$[K_\sigma] = \int_\Omega [\mathcal{B}]^T [S] [\mathcal{B}] \, d\Omega$$

The expression of mechanical force vectors, $\{F_P\}$, in Eq. 17 is given by

$$\{F_P\} = \int_\Omega \{\mathcal{W}\}^T P(x, y) \, d\Omega$$

in which

$$\{\mathcal{W}\}\{d\} = \sum_{i=1}^{9} \{\mathcal{W}_i\}\{q_i\}$$

where

$$\{\mathcal{W}_i\} = \begin{Bmatrix} 0 & 0 & N_i & 0 & 0 & 0 & 0 \end{Bmatrix}$$

similarly, hygrothermal loads, $\{F_{th}\}$ is expressed as

$$\{F_{th}\} = \int_\Omega [\mathcal{B}]^T \left\{\hat{F}\right\} d\Omega$$

III. Result and Discussion

In this section various examples have been taken to perform the dynamic analysis of laminated composite plate under hygrothermal environment. The computer code is developed on the basis of above mentioned finite element hygrothermal formulation. The transient analysis for various parameters are performed and the results and the discussions are presented.

A. Material Properties

Material properties used for the analysis are as follows

1) Material MM1 [15]: $E_1 = 40E_2$; $E_2 = 1 \times 10^6\, N/cm^2$; $G_{12} = 0.6E_2$; $G_{23} = 0.5E_2$, $\nu_{12} = \nu_{13} = \nu_{23} = 0.25$; $\rho = 8 \times 10^{-6} Ns^2/cm^4$
2) Material MM2 [16]: $E_2 = 21\, Gpa$, $E_1 = 525\, Gpa$ $G_{12} = G_{13} = G_{23} = 10.5\, Gpa, \nu_{12} = 0.25$ $\rho = 800\, kg/m^3$
3) Material MM3 [8] The various material properties are given for corresponding temperature variation in this subsection. Different material properties are considered for different temperature and moisture concentration. The material properties corresponding to various moisture concentration are listed in Table. 1, and corresponding to temperature are listed in Table. 2.

Table 1 Elastic modulus of carbon-epoxy lamina at different moisture concentration; $G_{12} = G_{13}, G_{23} = 0.4G_{12}, \beta_1 = 0, \beta_2 = 0.44$**.**

Elastic modulus (GPa)	Moisture Concentration, C %					
	0.25	0.50	0.75	1.00	1.25	1.50
E_1	172.5	172.5	172.5	172.5	172.5	172.5
E_2	6.72	6.54	6.36	6.17	6.17	6.17
G_{12}	3.45	3.45	3.45	3.45	3.45	3.45

Table 2 Elastic modulus of carbon-epoxy lamina at different temperature; $G_{13} = G_{12}$**,** $G_{23} = 0.4G_{12}$**,** $\alpha_1 = -0.3 \times 10^{-6}/K$**,** $\alpha_2 = 28.1 \times 10^{-6}/K$**.**

Elastic modulus (GPa)	Temperature $T\,(K)$					
	300	325	350	375	400	425
E_1	172.5	172.5	172.5	172.5	172.5	172.5
E_2	6.9	6.17	5.81	5.45	5.08	4.9
G_{12}	3.45	3.45	3.16	2.88	2.73	2.59

B. Boundary Condition

Various boundary conditions used for the analysis are as follows

- Simply Supported condition $(SS1)$
  - Edge parallel to x-axis: $u_0 = w_0 = \theta_x = \phi_x = 0$
  - Edge parallel to y-axis: $v_0 = w_0 = \theta_y = \phi_y = 0$
- Simply Supported condition $(SS2)$
  - Edge parallel to x-axis: $u_0 = v_0 = w_0 = \theta_x = \phi_x = 0$
  - Edge parallel to y-axis: $u_0 = v_0 = w_0 = \theta_y = \phi_y = 0$

C. Various Types of Blast Loading

The study of various blast loading effect on the structure is essential for structural analysis. In this section various kind of blast loads are defined.

- Step Loading

$$F(t) = \left\{ \begin{array}{cc} 1, & 0 \leq t \leq t_1 \\ 0, & t \geq t_1 \end{array} \right\}$$

where t_1 is the positive phase duration of load.

- Sinusoidal loading

$$F(t) = \left\{ \begin{array}{cc} sin(\pi t/t_1), & 0 \leq t \leq t_1 \\ 0, & t \geq t_1 \end{array} \right\}$$

- Explosive Blast Loading

$$F(t) = \left\{ \begin{array}{cc} e^{-\gamma t}, & 0 \leq t \leq t_1 \\ 0, & t \geq t_1 \end{array} \right\}$$

γ is the decay parameter, for the current analysis $\gamma = 660$

- Triangular Loading

$$F(t) = \left\{ \begin{array}{cc} 1 - t/t_1, & 0 \leq t \leq t_1 \\ 0, & t \geq t_1 \end{array} \right\}$$

The spatial pressure applied for the analysis are defined by

$$q(x_1, x_2, t) = q_0 sin(\pi x_1/a) sin(\pi x_2/b) F(t), \quad \text{Sinusoidal Load}$$

$$q(x_1, x_2, t) = q_0 F(t), \quad \text{Uniformly Distributed Load}$$

D. Transient Analysis

Various transient problems are analyzed and the obtained results are compared with the available solution to validate the present method. After validation some new results are presented. Transient response for laminated plates subjected to hygrothermal environment is computed applying Newmark's constant average acceleration method [17].

1. Transient Analysis of Orthotropic Plate

In this subsection, an orthotropic plate under suddenly applied step loading and the uniformly distributed spatial pressure distribution for simply supported boundary condition is considered. The side-Length, $a = b = 0.25\,m$ and side-to-thickness ratio, $a/h = 50$ are considered for the analysis. The material properties used for the analysis is MM2. The other parameters taken for the analysis are $q_0 = 1\,Mpa$, $t_1 = 2e^{-3}\,s$, and $\Delta t = 10^{-6}\,s$ for the dynamic analysis. The transverse displacement response is shown in the Fig.2. The results obtained are compared with the available literature [15] and found to be in well agreement.

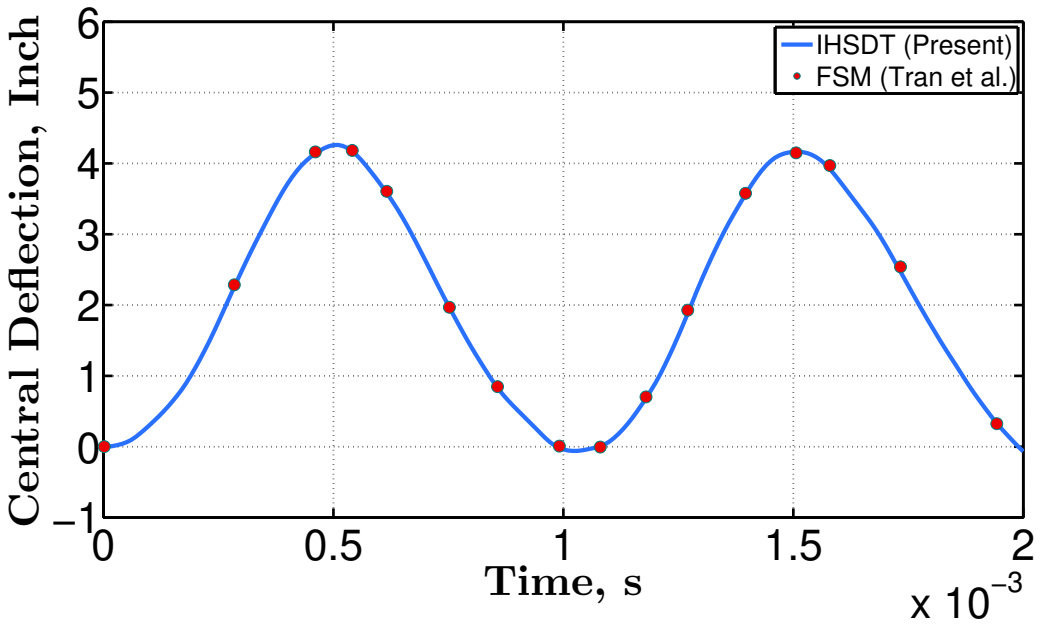

Fig. 2 Transverse displacement of an orthotropic plate under step uniform load with intensity $1\,MPa$**.**

2. Transient analysis of cross-ply laminated composite plate

In this subsection, a cross-ply $[0^0/90^0/0^0]$ laminated square plate under suddenly applied sin blast loading for the sinusoidal spatial pressure distribution is considered for the validation purpose of the present analysis. Length and total thickness of the plate are $a = b = 20\,in$ and $h = 1\,in$. Each lamina is assumed to be of the same thickness and is idealized as a homogeneous orthotropic material with the material properties MM1 in the principal material coordinate system. The other parameters such as $q_0 = 1000\ psi$ and $t_1 = 0.003\,s$ have been used by taking time step $\Delta t = 1e^{-5}\,s$. The transverse displacement response is shown in the Fig.3. The obtained results are compared with the available literature [16] and found to be in well agreement.

3. Transient Analysis of Laminated Composite Plate Under Hygrothermal Environment

After validation of present transient solutions for the mechanical load, in this section the response is calculated and compared for the hygrothermal load. A ten-layered simply supported cross-ply $[0^0/90^0]_{10}$ laminated composite plate under hygrothermal temperature is considered for the transient analysis. The material properties used for the analysis are $MM3$. The laminated composite plate consists of side-length $a = b = 0.5\,m$ and thickness $h = 5\,mm$. The impulse load with magnitude $q_0 = 100\ N/m^2$ is applied for time $t_1 = 0.003\,s$. The initial temperature $T_0 = 300\,K$ and time step of $\Delta t = 10e^{-6}\,s$ are considered. The present obtained results for temperature $T = 400\,K$ is presented in Fig.4. It is observed that the obtained results are in well agreement with the available solution[8]. The same problem is analyzed for the 1 % moisture concentration and the obtained response is presented in Fig.5. The result is compared with the available solution [8] and found to be in well agreement.

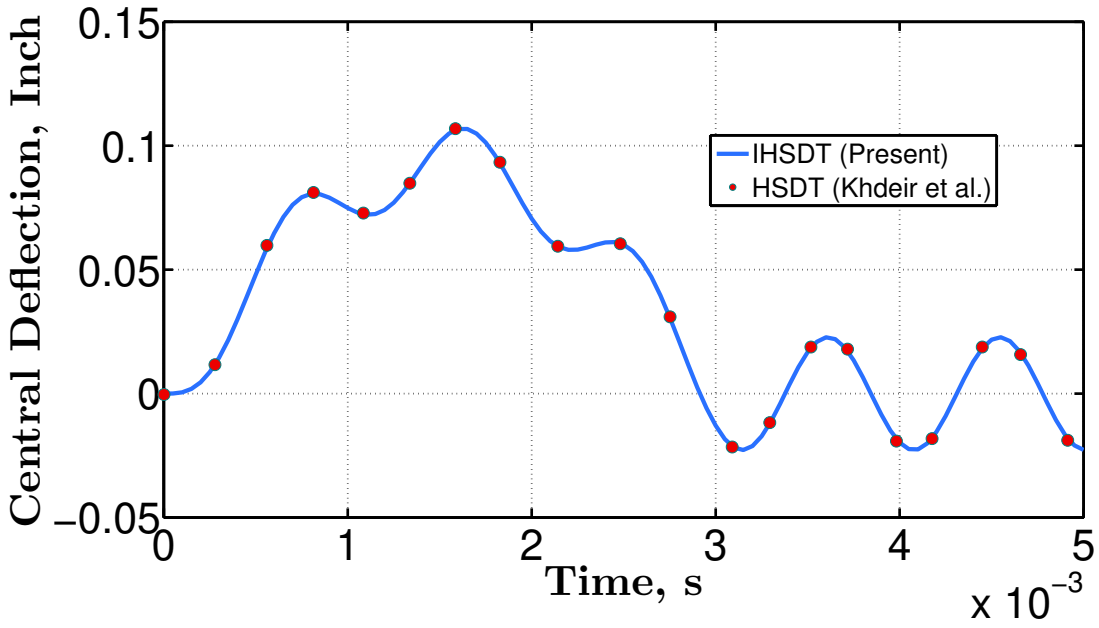

Fig. 3 Transverse displacement of symmetric cross-ply laminate $[0^0/90^0/0^0]$ plate subjected to sine pulse loading under simply supported boundary condition.

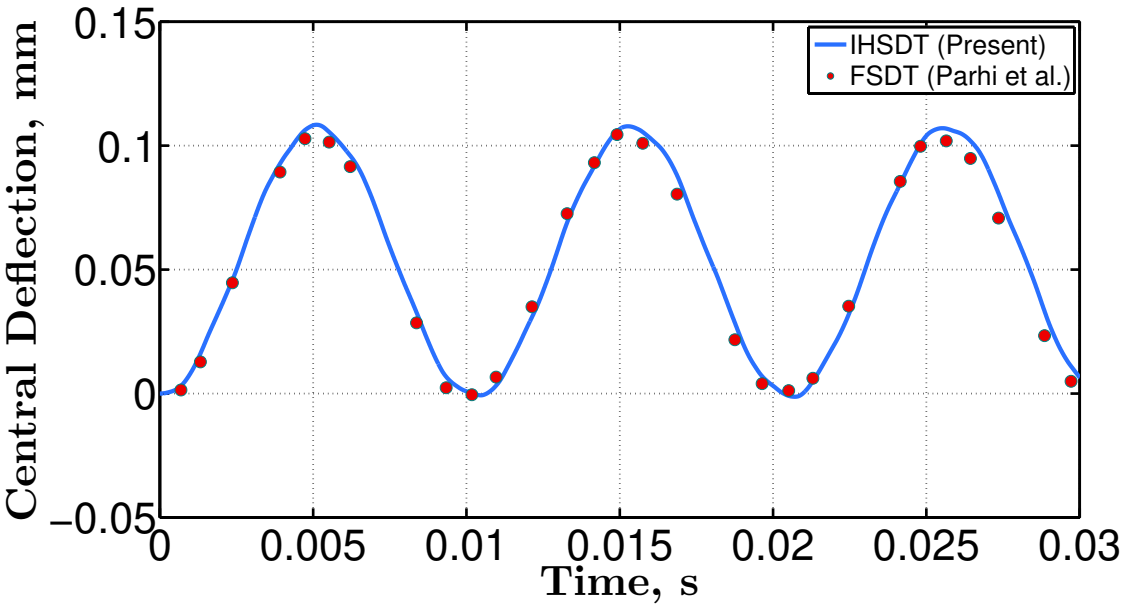

Fig. 4 Central deflection of ten-layered cross-ply laminate $[0^0/90^0]_{10}$ plate subjected to uniformly distributed spatial and thermal load with step time-dependent loading under simply supported boundary condition for temperature, $T = 400\,K$.

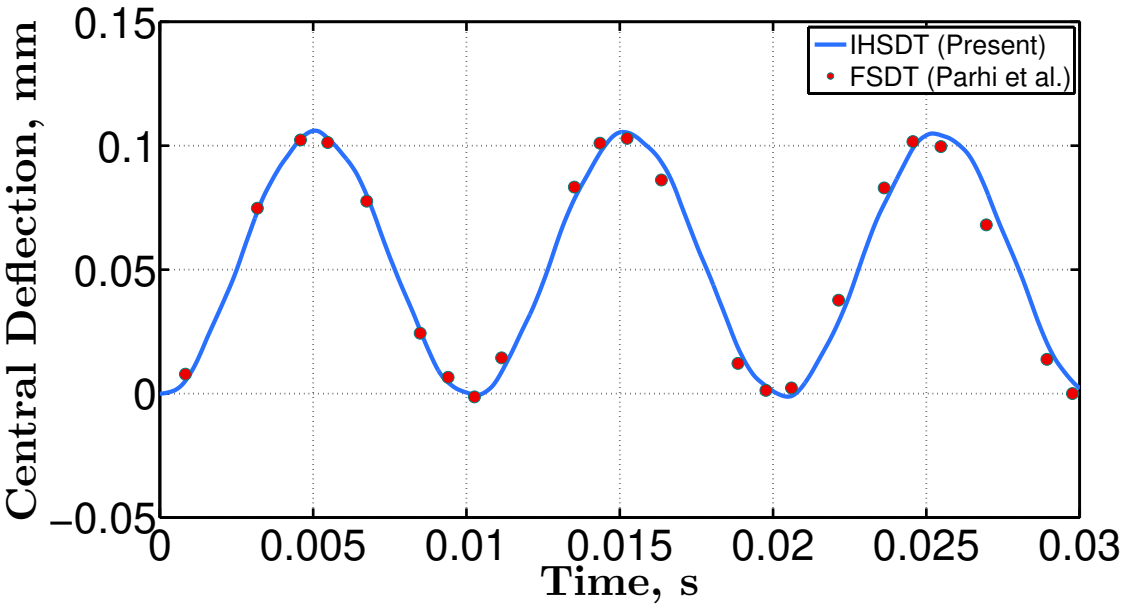

Fig. 5 Central deflection of ten-layered cross-ply laminate $[0^0/90^0]_{10}$ plate subjected to uniformly distributed spatial and hygrothermal load with step time-dependent load under simply supported boundary condition for moisture concentration, $C = 1\,\%$.

A four-layered cross-ply $[0^0/90^0]_2$ laminated plate of side-length, $a = b = 0.5\,m$ and side-to-thickness ratio, $a/h = 100$ is analyzed for various kinds of time-dependent load. The transient responses for the same are comparatively studied and presented in Fig. 6 for step, sinusoidal, triangular, and exponential blast load . The analysis is carried out for sinusoidal spatial load with $\Delta t = 10^{-6}\,s$ and $t_1 = 0.03\,s$ under simply supported boundary condition at temperature, $T = 400\,K$. It is observed that the central deflection due to step impulse load is more than the other mentioned load and exponential load causes least central deflection as evident from the Fig. 6.

The effects of number of layers on the transient analysis of laminated composite plate have also been investigated under thermal environment. The step load is considered for the analysis of cross-ply $[0^0/90^0]_n$ laminated plate where $n = 2$, 3, and 4. The obtained response is presented in Fig.7. It is observed that as number of layers increases the central deflection decreases and no significant change is found after increase in number of layer beyond four. Figure. 8 presents the effect of side-to-thickness ratio, $(a/h = 10, 20, 30, 50)$ on the thermal transient analysis of four-layered cross-ply $[0^0/90^0/90^0/0^0]$ laminated composite plate. The sinusoidal spatial load with step time-dependent load is considered for the transient analysis. It is observed that as side-to-thickness ratio, a/h, increases the central deflection also increases.

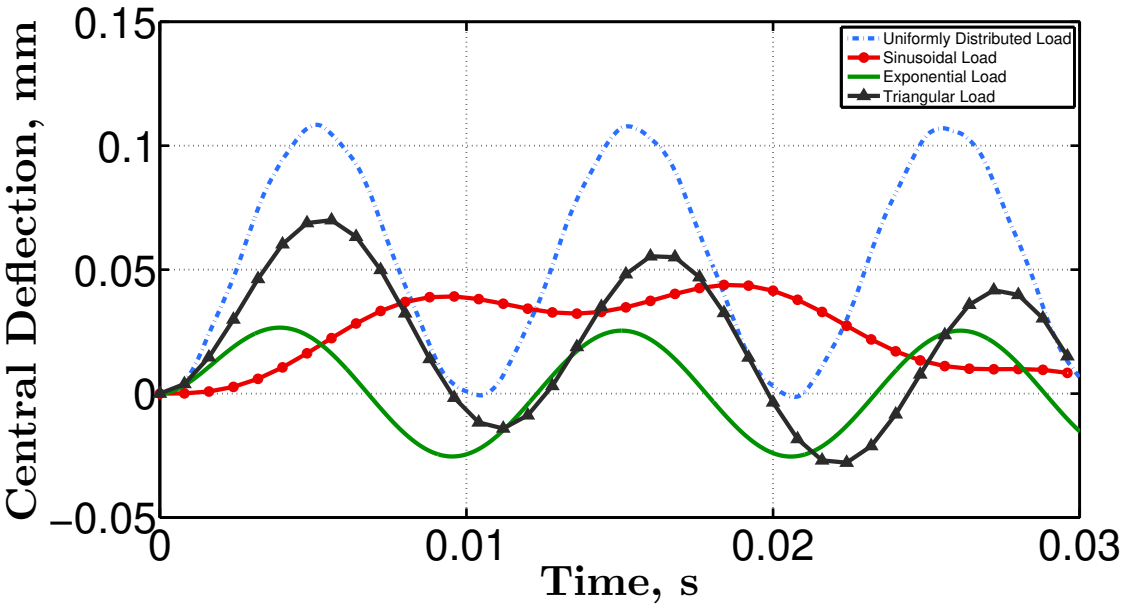

Fig. 6 Central deflection of four-layered cross-ply laminate $[0^0/90^0]_2$ plate subjected to various kinds of time-dependent load under simply supported boundary condition.

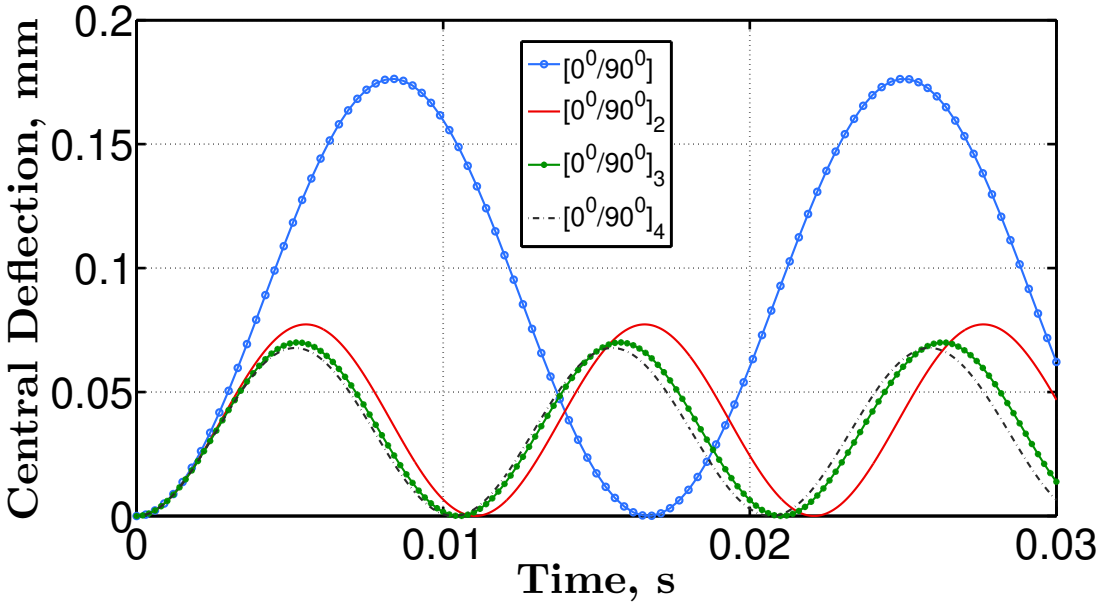

Fig. 7 Central deflection of cross-ply laminate plate subjected to uniformly distributed spatial load and time-dependent step load under simply supported boundary condition.

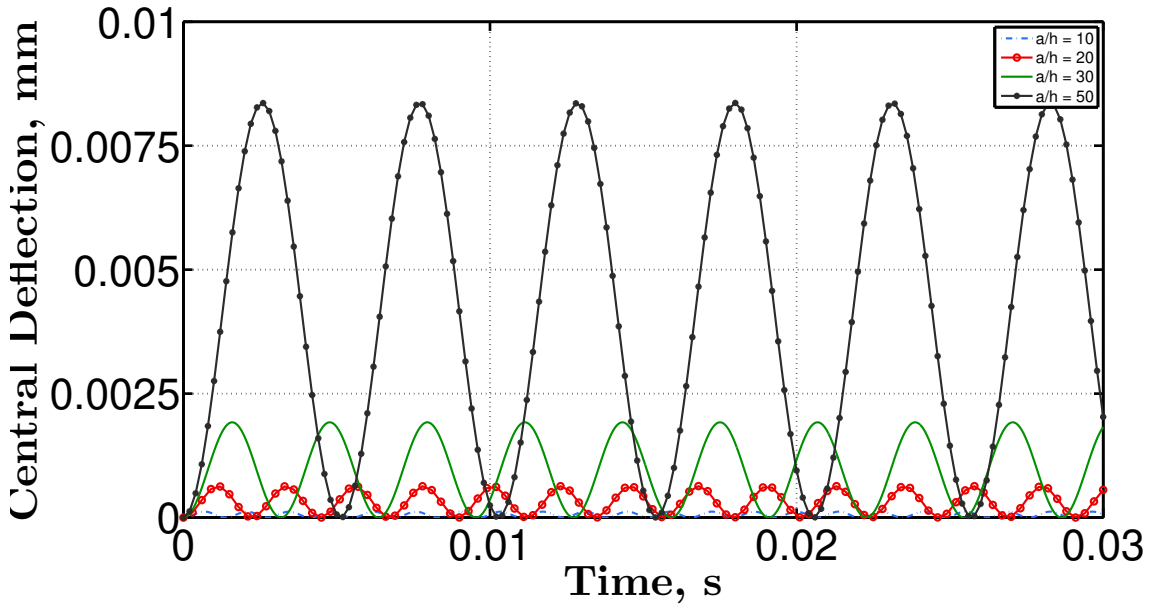

Fig. 8 Central deflection of cross-ply laminate $[0^0/90^0/90^0/0^0]$ plate subjected to sinusoidal spatial load and time-dependent step load under simply supported boundary condition for different side-to-thickness ratio.

IV. Conclusion

The transient analysis of laminated composite plate based on nonpolynomial shear deformation theory (NPSDT) under hygrothermal environment is carried out. The inverse hyperbolic shear deformation theory (IHSDT) along with Newmark's integration scheme is employed to solve the transient problems. To show the efficacy and wider applicability of present approach several types of examples are carried out. The results have been validated from the available solution in the literature. In this present study, the effect of various type of load, such as step, sinusoidal, triangular, and exponential blast load are investigated. Also, the effect of different side-to-thickness ratio and the number of layers on transient response in hygrothermal environment are analyzed.

Several novel results have been presented for the hygrothermal transient analysis of laminated composite plates. As no results have been reported in the literature using the present methodology for transient analysis and therefore the gap is rightly filled with the standard solution to provide a reference for the further analysis.

Appendix

$$[S] = \begin{bmatrix} S_{11} & 0 & S_{13} & S_{14} & 0 & S_{16} & S_{17} & 0 & S_{19} & 0 & S_{111} & 0 & S_{113} \\ & S_{22} & S_{23} & 0 & S_{25} & S_{26} & 0 & S_{28} & S_{29} & S_{210} & 0 & S_{112} & 0 \\ & & S_{33} & S_{34} & S_{35} & S_{36} & S_{37} & S_{38} & S_{39} & S_{310} & S_{311} & S_{312} & S_{313} \\ & & & S_{44} & 0 & S_{46} & S_{47} & 0 & S_{49} & 0 & S_{411} & 0 & S_{413} \\ & & & & S_{55} & S_{56} & 0 & S_{58} & S_{59} & S_{510} & 0 & S_{512} & 0 \\ & & & & & S_{66} & S_{67} & S_{68} & S_{69} & S_{610} & S_{611} & S_{612} & S_{613} \\ & & & & & & S_{77} & 0 & S_{79} & 0 & S_{711} & 0 & S_{713} \\ & & & & & & & S_{88} & S_{89} & S_{810} & 0 & S_{812} & 0 \\ & & & & & & & & S_{99} & S_{910} & S_{911} & S_{912} & S_{913} \\ & & & & & & & & & 0 & 0 & 0 & 0 \\ & & & & & & & & & & 0 & 0 & 0 \\ & & & & & & & & & & & 0 & 0 \\ & & & & & & & & & & & & 0 \end{bmatrix}$$

where

$S_{11} = N_x$, $S_{22} = N_y$, $S_{33} = N_x + N_y$, $S_{13} = S_{23} = N_{xy}$, $S_{210} = S_{311} = N_{yz}$, $S_{111} = S_{310} = N_{xz}$,
$S_{44} = R_x$, $S_{55} = R_y$, $S_{66} = R_x + R_y$, $S_{46} = S_{56} = R_{xy}$, $S_{212} = S_{313} = R_{yz}$, $S_{113} = R_{xz}$,
$S_{77} = F_x$, $S_{88} = F_y$, $S_{99} = F_x + F_y$, $S_{79} = S_{89} = F_{xy}$,
$S_{14} = -M_x$, $S_{34} = S_{35} = S_{16} = S_{26} = -M_{xy}$, $S_{25} = -M_y$, $S_{36} = -M_x - M_y$, $S_{411} = S_{610} = -M_{xz}$, $S_{510} = S_{611} = -M_{yz}$,
$S_{17} = P_x$, $S_{28} = P_y$, $S_{37} = S_{38} = S_{19} = S_{29} = P_{xy}$, $S_{39} = P_x + P_y$, $S_{312} = S_{711} = S_{910} = P_{xz}$, $S_{810} = S_{911} = P_{yz}$,
$S_{47} = -L_x$, $S_{58} = -L_y$, $S_{69} = -L_x - L_y$, $S_{67} = S_{68} = S_{49} = S_{59} = -L_{xy}$,
$S_{413} = S_{612} = -V_{xz}$, $S_{512} = S_{613} = -V_{yz}$,
$S_{713} = S_{912} = U_{xz}$, $S_{812} = S_{913} = U_{yz}$.

in which

$$\begin{Bmatrix} N_x \\ N_y \\ N_{xy} \end{Bmatrix} = \int \begin{Bmatrix} \sigma_x \\ \sigma_y \\ \sigma_{xy} \end{Bmatrix} dz; \quad \begin{Bmatrix} M_x \\ M_y \\ M_{xy} \end{Bmatrix} = \int \begin{Bmatrix} \sigma_x \\ \sigma_y \\ \sigma_{xy} \end{Bmatrix} z dz; \quad \begin{Bmatrix} P_x \\ P_y \\ P_{xy} \end{Bmatrix} = \int \begin{Bmatrix} \sigma_x \\ \sigma_y \\ \sigma_{xy} \end{Bmatrix} f(z) dz$$

$$\begin{Bmatrix} N_{yz} \\ N_{xz} \end{Bmatrix} = \int \begin{Bmatrix} \sigma_{yz} \\ \sigma_{xz} \end{Bmatrix} dz; \quad \begin{Bmatrix} M_{yz} \\ M_{xz} \end{Bmatrix} = \int \begin{Bmatrix} \sigma_{yz} \\ \sigma_{xz} \end{Bmatrix} z dz; \quad \begin{Bmatrix} P_{yz} \\ P_{xz} \end{Bmatrix} = \int \begin{Bmatrix} \sigma_{yz} \\ \sigma_{xz} \end{Bmatrix} f(z) dz$$

$$\begin{Bmatrix} R_x \\ R_y \\ R_{xy} \end{Bmatrix} = \int \begin{Bmatrix} \sigma_x \\ \sigma_y \\ \sigma_{xy} \end{Bmatrix} z^2 dz; \quad \begin{Bmatrix} L_x \\ L_y \\ L_{xy} \end{Bmatrix} = \int \begin{Bmatrix} \sigma_x \\ \sigma_y \\ \sigma_{xy} \end{Bmatrix} z f(z) dz; \quad \begin{Bmatrix} F_x \\ F_y \\ F_{xy} \end{Bmatrix} = \int \begin{Bmatrix} \sigma_x \\ \sigma_y \\ \sigma_{xy} \end{Bmatrix} (f(z))^2 dz$$

$$\begin{Bmatrix} R_{yz} \\ R_{xz} \end{Bmatrix} = \int \begin{Bmatrix} \sigma_{yz} \\ \sigma_{xz} \end{Bmatrix} f'(z) dz; \quad \begin{Bmatrix} U_{yz} \\ U_{xz} \end{Bmatrix} = \int \begin{Bmatrix} \sigma_{yz} \\ \sigma_{xz} \end{Bmatrix} f'(z) f(z) dz; \quad \begin{Bmatrix} V_{yz} \\ V_{xz} \end{Bmatrix} = \int \begin{Bmatrix} \sigma_{yz} \\ \sigma_{xz} \end{Bmatrix} z f'(z) dz$$

References

[1] Whitney, J., and Ashton, J., "Effect of environment on the elastic response of layered composite plates," *AIAA Journal*, Vol. 9, No. 9, 1971, pp. 1708–1713.

[2] Ram, K. S., and Sinha, P., "Hygrothermal effects on the free vibration of laminated composite plates," *Journal of Sound and Vibration*, Vol. 158, No. 1, 1992, pp. 133–148.

[3] Patel, B., Ganapathi, M., and Makhecha, D., "Hygrothermal effects on the structural behaviour of thick composite laminates using higher-order theory," *Composite Structures*, Vol. 56, No. 1, 2002, pp. 25–34.

[4] Rao, V., and Sinha, P., "Dynamic response of multidirectional composites in hygrothermal environments," *Composite Structures*, Vol. 64, No. 3-4, 2004, pp. 329–338.

[5] Singha, M. K., Ramachandra, L., and Bandyopadhyay, J., "Vibration behavior of thermally stressed composite skew plate," *Journal of sound and vibration*, Vol. 296, No. 4-5, 2006, pp. 1093–1102.

[6] Rath, M., and Sahu, S., "Vibration of woven fiber laminated composite plates in hygrothermal environment," *Journal of vibration and control*, Vol. 18, No. 13, 2012, pp. 1957–1970.

[7] Li, W., and Li, Y., "Vibration and sound radiation of an asymmetric laminated plate in thermal environments," *Acta Mechanica Solida Sinica*, Vol. 28, No. 1, 2015, pp. 11–22.

[8] Parhi, P., Bhattacharyya, S., , and Sinha, P., "Hygrothermal effects on the dynamic behavior of multiple delaminated composite plates and shells," *Journal of Sound and Vibration*, Vol. 248, No. 2, 2001, pp. 195–214.

[9] Shen, H.-S., Zheng, J.-J., and Huang, X.-L., "The effects of hygrothermal conditions on the dynamic response of shear deformable laminated plates resting on elastic foundations," *Journal of reinforced plastics and composites*, Vol. 23, No. 10, 2004, pp. 1095–1113.

[10] Makhecha, D., Ganapathi, M., and Patel, B., "Dynamic analysis of laminated composite plates subjected to thermal/mechanical loads using an accurate theory," *Composite Structures*, Vol. 51, No. 3, 2001, pp. 221–236.

[11] Panda, H., Sahu, S., and Parhi, P., "Hygrothermal effects on free vibration of delaminated woven fiber composite plates–numerical and experimental results," *Composite Structures*, Vol. 96, 2013, pp. 502–513.

[12] Wang, D., Xie, M., and Li, Y., "High-frequency dynamic analysis of plates in thermal environments based on energy finite element method," *Shock and Vibration*, Vol. 2015, 2015.

[13] Grover, N., Singh, B., and Maiti, D., "Analytical and finite element modeling of laminated composite and sandwich plates: An assessment of a new shear deformation theory for free vibration response," *International Journal of Mechanical Sciences*, Vol. 67, 2013, pp. 89–99.

[14] Bhavikatti, S. S., *Finite element analysis*, New Age International, New Delhi, 2005.

[15] Tran, L. V., Lee, J., Nguyen-Van, H., Nguyen-Xuan, H., and Wahab, M. A., "Geometrically nonlinear isogeometric analysis of laminated composite plates based on higher-order shear deformation theory," *International Journal of Non-Linear Mechanics*, Vol. 72, 2015, pp. 42–52.

[16] Khdeir, A., "Transient response of refined cross-ply laminated plates for various boundary conditions," *The Journal of the Acoustical Society of America*, Vol. 97, No. 3, 1995, pp. 1664–1669.

[17] Gupta, A., and Ghosh, A., "Transient Analysis of Anti-symmetric Cross-Ply and Angle-Ply Laminated Composite Plates Using Nurbs-Based Isogeometric Analysis," *58th AIAA/ASCE/AHS/ASC Structures, Structural Dynamics, and Materials Conference*, 2017, p. 1980.